

Why Do Adversarial Attacks Transfer? Explaining Transferability of Evasion and Poisoning Attacks

Ambra Demontis
DIEE, University of Cagliari, Italy

Marco Melis
DIEE, University of Cagliari, Italy

Maura Pintor
DIEE, University of Cagliari, Italy

Matthew Jagielski
Northeastern University, Boston, MA

Battista Biggio
DIEE, University of Cagliari, Italy
Pluribus One

Alina Oprea
Northeastern University, Boston, MA

Cristina Nita-Rotaru
Northeastern University, Boston, MA

Fabio Roli
DIEE, University of Cagliari, Italy
Pluribus One

ABSTRACT

Transferability captures the ability of an attack against a machine-learning model to be effective against a different, potentially unknown, model. Studying transferability of attacks has gained interest in the last years due to deployment of cyber-attack detection services based on machine learning. For these applications of machine learning, service providers avoid disclosing information about their machine-learning algorithms. As a result, attackers trying to bypass detection are forced to craft their attacks against a surrogate model instead of the actual target model used by the service. While previous work has shown that finding test-time transferable attack samples is possible, it is not well understood how an attacker may construct adversarial examples that are likely to transfer against different models, in particular in the case of training-time poisoning attacks. In this paper, we present the first empirical analysis aimed to investigate the transferability of both test-time evasion and training-time poisoning attacks. We provide a unifying, formal definition of transferability of such attacks and show how it relates to the input gradients of the surrogate and of the target classification models. We assess to which extent some of the most well-known machine-learning systems are vulnerable to transfer attacks, and explain why such attacks succeed (or not) across different models. To this end, we leverage some interesting connections highlighted in this work among the adversarial vulnerability of machine-learning models, their regularization hyperparameters and input gradients.

1 INTRODUCTION

The wide adoption of machine learning (ML) and deep learning algorithms in many critical applications introduces strong incentives for motivated adversaries to manipulate the results and models generated by these algorithms. Attacks against machine learning systems can happen during multiple stages in the learning pipeline. For instance, in many settings training data is collected online and thus can not be fully trusted. In *poisoning availability attacks*, the attacker controls a certain amount of training data, thus influencing the trained model and ultimately the predictions at testing time on most points in testing set [4, 16, 18, 26–28, 33, 35, 40, 46]. *Poisoning integrity attacks* have the goal of modifying predictions on a few targeted points by manipulating the training process [18, 40].

On the other hand, *evasion attacks* involve small manipulations of testing data points that results in misprediction at testing time on those points [3, 7, 9, 13, 30, 37, 41, 44, 47].

Creating poisoning and evasion attack points is not a trivial task, particularly when many online services avoid disclosing information about their machine learning algorithms. As a result, attackers are forced to craft their attacks in *black-box* settings, against a surrogate model instead of the real model used by the service, hoping that the attack will be effective on the real model. The *transferability* property of an attack is satisfied when an attack developed for a particular machine learning model (i.e., a surrogate model) is also effective against the target model. Attack transferability was observed in early studies on adversarial examples [13, 41] and has gained a lot more interest in recent years with the advancement of machine learning cloud services. Previous work has reported empirical findings about the transferability of evasion attacks [3, 12, 13, 19, 24, 30, 31, 41, 42, 45] and, only recently, also on the transferability of poisoning integrity attacks [40]. In spite of these efforts, the question of *when and why do adversarial points transfer* remains largely unanswered.

In this paper we present the first comprehensive evaluation of transferability of evasion and poisoning availability attacks, understanding the factors contributing to transferability of both attacks. In particular, we consider attacks crafted with gradient-based optimization techniques (e.g., [4, 7, 21]), a popular and successful mechanism used to create attack data points. We unify for the first time evasion and poisoning attacks into an optimization framework that can be instantiated for a range of threat models and adversarial constraints. We provide a formal definition of transferability and show that, under linearization of the loss function computed under attack, several main factors impact transferability: the *intrinsic adversarial vulnerability* of the target model, the *complexity* of the surrogate model used to optimize the attacks, and its alignment with the target model. Furthermore, we derive a new poisoning attack for logistic regression, and perform a comprehensive evaluation of both evasion and poisoning attacks on multiple datasets, confirming our theoretical analysis.

In more detail, the contributions of our work are:

Optimization framework for evasion and poisoning attacks.. We introduce a unifying framework based on gradient-descent optimization that encompasses both evasion and poisoning attacks.

Our framework supports threat models with different adversarial goals (integrity and availability), amount of knowledge available to the adversary (white-box and black-box), as well as different adversarial capabilities (causative or exploratory). Our framework generalizes existing attacks proposed by previous work for evasion [3, 7, 13, 21, 41] and poisoning [4, 16, 18, 22, 25, 46]. Under our framework, we derive a novel gradient-based poisoning availability attack against logistic regression. We remark here that poisoning attacks are more difficult to derive than evasion ones, as they require computing hypergradients from a bilevel optimization problem, to capture the dependency on how the machine-learning model changes while the training poisoning points are modified [4, 16, 18, 22, 25, 46].

Transferability definition and theoretical bound.. We give a formal definition of transferability of evasion and poisoning attacks and an upper bound on a transfer attack’s success, which allows us to derive three metrics connected to *model complexity*. Our formal definition unveils that transferability depends on: (1) size of input gradients of the target classifier; (2) how well the gradients of the surrogate and target models align; and (3) the variance of the loss landscape used for the attacker objective to generate the attack points.

Comprehensive experimental evaluation of transferability.. We consider a wide range of classifiers, including logistic regression, SVM with both linear and RBF kernels, ridge regression, random forests, and deep neural networks (both feed-forward and convolutional neural networks), all with different hyperparameter settings to reflect different model complexities. We evaluate the transferability of our attacks on three datasets related to different applications: handwritten digit recognition (MNIST), Android malware detection (DREBIN), and face recognition (LFW). We confirm our theoretical analysis for both evasion and poisoning attacks.

Insights into transferability.. We demonstrate that attack transferability depends strongly on *model complexity* for the target model and, thus, the inherent vulnerability of the target model. Reducing the size of input gradients, via, for instance, regularization, may allow us to learn more robust classifiers for both evasion and poisoning availability attacks. Second, transferability is also impacted by the surrogate model’s alignment with the target model. Surrogates with better alignments to their targets (in terms of the cosine angle between their gradients) are more successful at transferring the attack points. Third, surrogate loss functions that are more stable and have lower variance tend to facilitate gradient-based optimization attacks to find better local optima (see Figure 1). As less complex models exhibit lower variance of their loss function, they typically result in better surrogates.

Organization.. We discuss background on threat modeling against machine learning in Section 2. We introduce our unifying optimization framework for evasion and poisoning attacks, as well as the poisoning attack for logistic regression in Section 3. We then formally define transferability for both evasion and poisoning attacks, and show its approximate connection with the input gradients used to craft the corresponding attack samples (Section 4). Experiments are reported in Section 5, highlighting connections among regularization hyperparameters, the size of input gradients, and transferability of attacks, on different case studies involving handwritten

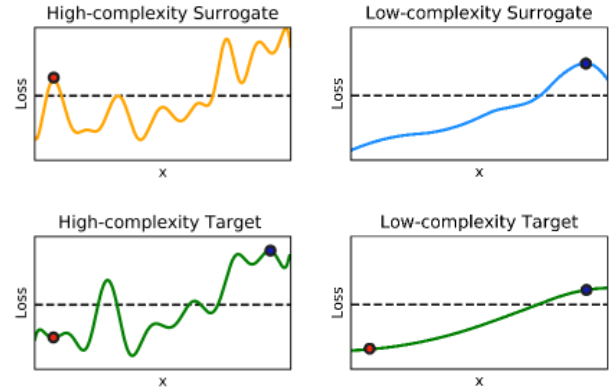


Figure 1: Conceptual representation of transferability. We show the loss function of the attack objective as a function of a single feature x . The top row includes 2 surrogate models (High and Low Complexity), while the bottom row includes both models as targets. The adversarial samples are represented as red dots for High-Complexity Surrogate and blue dots for Low-Complexity Surrogate. If the adversarial sample loss is below a certain threshold (represented as a black horizontal line), the point is correctly classified, otherwise it is wrongly classified. The adversarial point computed against the High-Complexity model (top left) lays in a local optimum due to the irregularity of the objective function. This point is not effective even against the same classifier trained on a different dataset (bottom left) due to the variance of High-Complexity classifier. The adversarial point computed against the Low Complexity model (top right), instead, succeeds against both Low and High-Complexity targets (left and right bottom, respectively).

digit recognition, Android malware detection, and face recognition. We discuss related work in Section 6 and conclude in Section 7.

2 BACKGROUND AND THREAT MODEL

Supervised learning includes: (1) a training phase in which training data is given as input to a learning algorithm, resulting in a trained ML model; (2) a testing phase in which the model is applied to new data and a prediction is generated. In this paper, we consider a range of adversarial models against machine learning classifiers at both training and testing time. Attackers are defined by: (i) their goal or objective in attacking the system; (ii) their knowledge of the system; (iii) their capabilities in influencing the system through manipulation of the input data. Before we detail each of these, we introduce our notation, and point out that the threat model and attacks considered in this work are suited to binary classification, but can be extended to multi-class settings.

Notation.. We denote the sample and label spaces with \mathcal{X} and $\mathcal{Y} \in \{-1, +1\}$, respectively, and the training data with $\mathcal{D} = (\mathbf{x}_i, y_i)_{i=1}^n$, where n is the training set size. We use $L(\mathcal{D}, \mathbf{w})$ to denote the loss incurred by classifier $f : \mathcal{X} \mapsto \mathcal{Y}$ (parameterized by \mathbf{w}) on \mathcal{D} . Typically, this is computed by averaging a loss function $\ell(y, \mathbf{x}, \mathbf{w})$ computed on each data point, i.e., $L(\mathcal{D}, \mathbf{w}) = \frac{1}{n} \sum_{i=1}^n \ell(y_i, \mathbf{x}_i, \mathbf{w})$.

We assume that the classifier f is learned by minimizing an objective function $\mathcal{L}(\mathcal{D}, \mathbf{w})$ on the training data. Typically, this is an estimate of the generalization error, obtained by the sum of the empirical loss L on training data \mathcal{D} and a regularization term.

2.1 Threat Model: Attacker’s Goal

We define the attacker’s goal based on the desired security violation. In particular, the attacker may aim to cause either an *integrity* violation, to evade detection without compromising normal system operation; or an *availability* violation, to compromise the normal system functionalities available to legitimate users.

2.2 Threat Model: Attacker’s Knowledge

We characterize the attacker’s knowledge κ as a tuple in an abstract knowledge space \mathcal{K} consisting of four main dimensions, respectively representing knowledge of: (k.i) the training data \mathcal{D} ; (k.ii) the feature set \mathcal{X} ; (k.iii) the learning algorithm f , along with the objective function \mathcal{L} minimized during training; and (k.iv) the parameters \mathbf{w} learned after training the model. This categorization enables the definition of many different kinds of attacks, ranging from *white-box* attacks with full knowledge of the target classifier to *black-box* attacks in which the attacker has limited information about the target system.

White-Box Attacks.. We assume here that the attacker has full knowledge of the target classifier, i.e., $\kappa = (\mathcal{D}, \mathcal{X}, f, \mathbf{w})$. This setting allows one to perform a worst-case evaluation of the security of machine-learning algorithms, providing empirical upper bounds on the performance degradation that may be incurred by the system under attack.

Black-Box Attacks.. We assume here that the input feature representation \mathcal{X} is known. For images, this means that we do consider pixels as the input features, consistently with other recent work on black-box attacks against machine learning [30, 31]. At the same time, the training data \mathcal{D} and the type of classifier f are not known to the attacker. We consider the most realistic attack model in which the attacker does not have querying access to the classifier.

The attacker can collect a surrogate dataset $\hat{\mathcal{D}}$, ideally sampled from the same underlying data distribution as \mathcal{D} , and train a *surrogate model* \hat{f} on such data to approximate the target function f . Then, the attacker can craft the attacks against \hat{f} , and then check whether they successfully *transfer* to the target classifier f . By denoting limited knowledge of a given component with the *hat* symbol, such black-box attacks can be denoted with $\hat{\kappa} = (\hat{\mathcal{D}}, \mathcal{X}, \hat{f}, \hat{\mathbf{w}})$.

2.3 Threat Model: Attacker’s Capability

This attack characteristic defines how the attacker can influence the system, and how data can be manipulated based on application-specific constraints. If the attacker can manipulate both training and test data, the attack is said to be *causative*. It is instead referred to as *exploratory*, if the attacker can only manipulate test data. These scenarios are more commonly known as *poisoning* [4, 16, 22, 25, 46] and *evasion* attacks [3, 7, 13, 41].

Another aspect related to the attacker’s capability depends on the presence of application-specific constraints on data manipulation. For instance, to evade malware detection, malicious code has to be

modified without compromising its intrusive functionality. This may be done against systems leveraging static code analysis, by injecting instructions or code that will never be executed [10, 14, 44]. These constraints can be generally accounted for in the definition of the optimal attack strategy by assuming that the initial attack sample \mathbf{x} can only be modified according to a space of possible modifications $\Phi(\mathbf{x})$.

3 OPTIMIZATION FRAMEWORK FOR GRADIENT-BASED ATTACKS

We introduce here a general optimization framework that encompasses both evasion and poisoning attacks. White-box gradient attacks have been considered for evasion (e.g., [3, 7, 13, 21, 41]) or poisoning attacks (e.g., [4, 16, 22, 25]) in previous work. Our optimization framework not only unifies existing evasion and poisoning attacks, but it also enables the design of new attacks. After defining our general formulation, we instantiate it for evasion and poisoning attacks, and use it to derive a new poisoning availability attack for logistic regression.

3.1 Gradient-based Optimization Algorithm

Given the attacker’s knowledge $\kappa \in \mathcal{K}$ and an attack sample $\mathbf{x}' \in \Phi(\mathbf{x})$ along with its label y , the attacker’s goal can be defined in terms of an objective function $\mathcal{A}(\mathbf{x}', y, \kappa) \in \mathbb{R}$ (e.g., a loss function) which measures how effective the attack sample \mathbf{x}' is. The optimal attack strategy can be thus given as:

$$\mathbf{x}^* \in \arg \max_{\mathbf{x}' \in \Phi(\mathbf{x})} \mathcal{A}(\mathbf{x}', y, \kappa). \quad (1)$$

Note that, for the sake of clarity, we consider here the optimization of a single attack sample, but this formulation can be easily extended to account for multiple attack points. In particular, in the case of poisoning attacks, the attacker maximizes his objective by finding *multiple poisoning points for insertion into the training data*.

Algorithm 1 provides a general gradient-ascent algorithm that can be used to solve the aforementioned problem for both evasion and poisoning attacks. It iteratively updates the attack sample along the gradient of the objective function, ensuring the resulting point to be within the feasible domain through a projection operator Π_Φ . The gradient step size η is determined in each update step with a line-search method based on bisection, to reduce the number of iterations required to reach a local or global optimum (depending on whether the objective function and the constraints are concave).

We finally remark that non-differentiable learning algorithms, like decision trees and random forests, can be attacked with more complex strategies [17, 29] or using the same algorithm against a differentiable surrogate learner.

3.2 Evasion Attacks

In evasion attacks, the attacker manipulates test samples to have them misclassified, i.e., to evade detection by a learning algorithm. For white-box evasion, the optimization problem given in Eq. (1)

Algorithm 1 Gradient-based Evasion and Poisoning Attacks

Input: \mathbf{x}, y : the input sample and its label; $\mathcal{A}(\mathbf{x}, y, \boldsymbol{\kappa})$: the attacker’s objective; $\boldsymbol{\kappa} = (\mathcal{D}, \mathcal{X}, f, \mathbf{w})$: the attacker’s knowledge parameter vector; $\Phi(\mathbf{x})$: the feasible set of manipulations that can be made on \mathbf{x} ; $t > 0$: a small number.

Output: \mathbf{x}' : the adversarial example.

- 1: Initialize the attack sample: $\mathbf{x}' \leftarrow \mathbf{x}$
 - 2: **repeat**
 - 3: Store attack from previous iteration: $\mathbf{x} \leftarrow \mathbf{x}'$
 - 4: Update step: $\mathbf{x}' \leftarrow \Pi_{\Phi}(\mathbf{x} + \eta \nabla_{\mathbf{x}} \mathcal{A}(\mathbf{x}, y, \boldsymbol{\kappa}))$, where the step size η is chosen with line search (bisection method), and Π_{Φ} ensures projection on the feasible domain Φ .
 - 5: **until** $|\mathcal{A}(\mathbf{x}', y, \boldsymbol{\kappa}) - \mathcal{A}(\mathbf{x}, y, \boldsymbol{\kappa})| \leq t$
 - 6: **return** \mathbf{x}'
-

can be rewritten as:

$$\max_{\mathbf{x}'} \quad \ell(y, \mathbf{x}', \mathbf{w}), \quad (2)$$

$$\text{s.t.} \quad \|\mathbf{x}' - \mathbf{x}\|_p \leq \varepsilon, \quad (3)$$

$$\mathbf{x}_{\text{lb}} \leq \mathbf{x}' \leq \mathbf{x}_{\text{ub}}, \quad (4)$$

where $\|\mathbf{v}\|_p$ is the ℓ_p norm of \mathbf{v} , and we assume that the classifier parameters \mathbf{w} are known. For the black-box case, it suffices to use the parameters $\hat{\mathbf{w}}$ of the surrogate classifier \hat{f} .

The intuition here is that the attacker maximizes the loss on the adversarial sample with the original class, to cause misclassification to the opposite class. The manipulation constraints $\Phi(\mathbf{x})$ are given in terms of: (i) a distance constraint $\|\mathbf{x}' - \mathbf{x}\|_p \leq \varepsilon$, which sets a bound on the maximum input perturbation between \mathbf{x} (i.e., the input sample) and the corresponding modified adversarial example \mathbf{x}' ; and (ii) a box constraint $\mathbf{x}_{\text{lb}} \leq \mathbf{x}' \leq \mathbf{x}_{\text{ub}}$ (where $\mathbf{u} \leq \mathbf{v}$ means that each element of \mathbf{u} has to be not greater than the corresponding element in \mathbf{v}), which bounds the values of the attack sample \mathbf{x}' .

For images, the former constraint is used to implement either *dense* or *sparse* evasion attacks [11, 23, 36]. Normally, the ℓ_2 and the ℓ_{∞} distances between pixel values are used to cause an indistinguishable image blurring effect (by slightly manipulating all pixels). Conversely, the ℓ_1 distance corresponds to a sparse attack in which only few pixels are significantly manipulated, yielding a salt-and-pepper noise effect on the image [11, 36]. The box constraint can be used to bound each pixel value between 0 and 255, or to ensure manipulation of only a specific region of the image. For example, if some pixels should not be manipulated, one can set the corresponding values of \mathbf{x}_{lb} and \mathbf{x}_{ub} equal to those of \mathbf{x} .

Maximum-confidence vs. minimum-distance evasion.. Our formulation of evasion attacks aims to produce adversarial examples that are misclassified with *maximum confidence* by the classifier, within the given space of feasible modifications. This is substantially different from crafting minimum-distance adversarial examples, as formulated in [41] and in follow-up work (e.g., [31]). This difference is conceptually depicted in Fig. 2. In particular, in terms of transferability, it is now widely acknowledged that higher-confidence attacks have better chances of successfully transferring to the target classifier (and even of bypassing countermeasures based on gradient masking) [2, 7, 12]. For this reason, in this work we consider

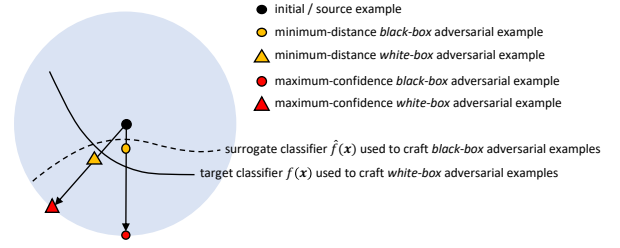


Figure 2: Conceptual representation of maximum-confidence evasion attacks (within an ℓ_2 ball of radius ε) vs. minimum-distance adversarial examples. Maximum-confidence attacks tend to transfer better than minimum-distance ones, as they are misclassified with higher confidence (although requiring more modifications).

evasion attacks that aim to craft adversarial examples misclassified with *maximum* confidence.

Initialization.. There is another factor known to improve transferability of evasion attacks, as well as their effectiveness in the white-box setting. It consists of running the attack starting from different initialization points to mitigate the problem of getting stuck in poor local optima [3, 12, 48]. In addition to starting the gradient ascent from the initial point \mathbf{x} , we also consider starting the gradient ascent from the projection of a randomly-chosen point of the opposite class onto the feasible domain. This helps finding better local optima, through the identification of more promising paths towards evasion [12, 45, 48].

3.3 Poisoning Availability Attacks

Poisoning attacks consist of manipulating training data (mainly by injecting adversarial points into the training set) to either favor intrusions without affecting normal system operation, or to purposely compromise normal system operation to cause a denial of service. The former are referred to as poisoning integrity attacks, while the latter are known as poisoning availability attacks [5, 46]. Recent work has mostly addressed transferability of poisoning integrity attacks [40], including backdoor attacks [8, 15]. In this work we focus on poisoning availability attacks, as their transferability properties have not yet been widely investigated. Crafting transferable poisoning availability attacks is much more challenging than crafting transferable poisoning integrity attacks, as the latter have a much more modest goal (modifying prediction on a small set of targeted points).

As for the evasion case, we formulate poisoning in a white-box setting, given that the extension to black-box attacks is immediate through the use of surrogate learners. Poisoning is formulated as a bilevel optimization problem in which the outer optimization maximizes the attacker’s objective \mathcal{A} (typically, a loss function L computed on untainted data), while the inner optimization amounts to learning the classifier on the poisoned training data [4, 22, 46].

This can be made explicit by rewriting Eq. (1) as:

$$\max_{\mathbf{x}'} L(\mathcal{D}_{\text{val}}, \mathbf{w}^*) = \sum_{j=1}^m \ell(y_j, \mathbf{x}_j, \mathbf{w}^*) \quad (5)$$

$$\text{s.t. } \mathbf{w}^* \in \arg \min_{\mathbf{w}} \mathcal{L}(\mathcal{D}_{\text{tr}} \cup (\mathbf{x}', y), \mathbf{w}) \quad (6)$$

where \mathcal{D}_{tr} and \mathcal{D}_{val} are the training and validation datasets available to the attacker. The former, along with the poisoning point \mathbf{x}' , is used to train the learner on poisoned data, while the latter is used to evaluate its performance on untainted data, through the loss function $L(\mathcal{D}_{\text{val}}, \mathbf{w}^*)$. Notably, the objective function implicitly depends on \mathbf{x}' through the parameters \mathbf{w}^* of the poisoned classifier.

The attacker's capability is limited by assuming that the attacker can inject only a small fraction α of poisoning points into the training set. Thus, the attacker solves an optimization problem involving a set of poisoned data points (αn) added to the training data.

Poisoning points can be optimized via gradient-ascent procedures, as shown in Algorithm 1. The main challenge is to compute the gradient of the attacker's objective (i.e., the validation loss) with respect to each poisoning point. In fact, this gradient has to capture the implicit dependency of the optimal parameter vector \mathbf{w}^* (learned after training) on the poisoning point being optimized, as the classification function changes while this point is updated. Provided that the attacker function is differentiable w.r.t. \mathbf{w} and \mathbf{x} , the required gradient can be computed using the chain rule [4, 5, 22, 25, 46]:

$$\nabla_{\mathbf{x}} \mathcal{A} = \nabla_{\mathbf{x}} L + \frac{\partial \mathbf{w}}{\partial \mathbf{x}}^\top \nabla_{\mathbf{w}} L, \quad (7)$$

where the term $\frac{\partial \mathbf{w}}{\partial \mathbf{x}}$ captures the implicit dependency of the parameters \mathbf{w} on the poisoning point \mathbf{x} . Under some regularity conditions, this derivative can be computed by replacing the inner optimization problem with its stationarity (Karush-Kuhn-Tucker, KKT) conditions, i.e., with its implicit equation $\nabla_{\mathbf{w}} \mathcal{L}(\mathcal{D}_{\text{tr}} \cup (\mathbf{x}', y), \mathbf{w}) = \mathbf{0}$ [22, 25]. By differentiating this expression w.r.t. the poisoning point \mathbf{x} , one yields:

$$\nabla_{\mathbf{x}} \nabla_{\mathbf{w}} \mathcal{L} + \frac{\partial \mathbf{w}}{\partial \mathbf{x}}^\top \nabla_{\mathbf{w}}^2 \mathcal{L} \in \mathbf{0}. \quad (8)$$

Solving for $\frac{\partial \mathbf{w}}{\partial \mathbf{x}}$, we obtain $\frac{\partial \mathbf{w}}{\partial \mathbf{x}}^\top = -(\nabla_{\mathbf{x}} \nabla_{\mathbf{w}} \mathcal{L})(\nabla_{\mathbf{w}}^2 \mathcal{L})^{-1}$, which can be substituted in Eq. (7) to obtain the required gradient:

$$\nabla_{\mathbf{x}} \mathcal{A} = \nabla_{\mathbf{x}} L - (\nabla_{\mathbf{x}_c} \nabla_{\mathbf{w}} \mathcal{L})(\nabla_{\mathbf{w}}^2 \mathcal{L})^{-1} \nabla_{\mathbf{w}} L. \quad (9)$$

Gradients for SVM.. Poisoning attacks for SVM were first proposed in [4]. Here, we report a simplified expression for SVM poisoning, with \mathcal{L} corresponding to the dual SVM learning problem, and L to the hinge loss (in the outer optimization):

$$\nabla_{\mathbf{x}_c} \mathcal{A} = -\alpha_c \frac{\partial \mathbf{k}_{kc}}{\partial \mathbf{x}_c} \mathbf{y}_k + \alpha_c \begin{bmatrix} \frac{\partial \mathbf{k}_{sc}}{\partial \mathbf{x}_c} & 0 \end{bmatrix} \begin{bmatrix} \mathbf{K}_{ss} & \mathbf{1} \\ \mathbf{1}^\top & 0 \end{bmatrix}^{-1} \begin{bmatrix} \mathbf{K}_{sk} \\ \mathbf{1}^\top \end{bmatrix} \mathbf{y}_k. \quad (10)$$

We use c , s and k here to respectively index the attack point, the support vectors, and the validation points for which $\ell(y, \mathbf{x}, \mathbf{w}) > 0$ (corresponding to a non-null derivative of the hinge loss). The coefficient α_c is the dual variable assigned to the poisoning point by the learning algorithm, and \mathbf{k} and \mathbf{K} contain kernel values between the corresponding indexed sets of points.

Gradients for Logistic Regression.. Logistic regression is a linear classifier that estimates the probability of the positive class using the sigmoid function. A poisoning attack against logistic regression has been derived in [22], but maximizing a different outer objective and not directly the validation loss. One of our contributions is to compute gradients for logistic regression under our optimization framework. Using logistic loss as the attacker's loss, the poisoning gradient for logistic regression can be computed as:

$$\nabla_{\mathbf{x}_c} \mathcal{A} = - \begin{bmatrix} \nabla_{\mathbf{x}_c} \nabla_{\boldsymbol{\theta}} \mathcal{L} \\ C \mathbf{z}_c \boldsymbol{\theta} \end{bmatrix}^\top \begin{bmatrix} \nabla_{\boldsymbol{\theta}}^2 \mathcal{L} & \mathbf{X} \mathbf{z}_c C \\ C \mathbf{z}_c \mathbf{X} & C \sum_i^n \mathbf{z}_i \end{bmatrix}^{-1} \begin{bmatrix} \mathbf{X}(\mathbf{y} \circ \boldsymbol{\sigma} - \mathbf{y}) \\ \mathbf{y}^\top (\boldsymbol{\sigma} - \mathbf{1}) \end{bmatrix} C,$$

where $\boldsymbol{\theta}$ are the classifier weights (bias excluded), \circ is the element-wise product, \mathbf{z} is equal to $\boldsymbol{\sigma}(1 - \boldsymbol{\sigma})$, $\boldsymbol{\sigma}$ is the sigmoid of the signed discriminant function (each element of that vector is therefore: $\sigma_i = \frac{1}{1 + \exp(-y_i f_i)}$ with $f_i = \mathbf{x}_i \boldsymbol{\theta} + b$), and:

$$\nabla_{\boldsymbol{\theta}}^2 \mathcal{L} = C \sum_i^n \mathbf{x}_i \mathbf{z}_i \mathbf{x}_i^\top + \mathbb{I}, \quad (11)$$

$$\nabla_{\mathbf{x}_c} \nabla_{\boldsymbol{\theta}} \mathcal{L} = C(\mathbb{I} \circ (y_c \boldsymbol{\sigma}_c - y_c) + \mathbf{z}_c \boldsymbol{\theta} \mathbf{x}_c^\top) \quad (12)$$

In the above equations, \mathbb{I} is the identity matrix.

4 TRANSFERABILITY DEFINITION AND METRICS

We discuss here an intriguing connection among transferability of both evasion and poisoning attacks, input gradients and regularization, and highlight the factors impacting transferability between a surrogate and a target model. For notational convenience, we denote in the following the attack points as $\mathbf{x}^* = \mathbf{x} + \hat{\boldsymbol{\delta}}$, where \mathbf{x} is the initial attack point and $\hat{\boldsymbol{\delta}}$ the adversarial perturbation optimized by the attack algorithm against the *surrogate* classifier, for both evasion and poisoning attacks. We start by formally defining transferability for evasion attacks, and then discuss how this definition and the corresponding metrics can be generalized to poisoning.

Transferability of Evasion Attacks.. Given an evasion attack point \mathbf{x}^* , crafted against a surrogate learner (parameterized by $\hat{\mathbf{w}}$), we define its *transferability* as the loss attained by the target classifier f (parameterized by \mathbf{w}) on that point, i.e., $T = \ell(y, \mathbf{x} + \hat{\boldsymbol{\delta}}, \mathbf{w})$. This can be simplified through a linear approximation of the loss function, which reasonably holds for sufficiently-small input perturbations:

$$T = \ell(y, \mathbf{x} + \hat{\boldsymbol{\delta}}, \mathbf{w}) \approx \ell(y, \mathbf{x}, \mathbf{w}) + \hat{\boldsymbol{\delta}}^\top \nabla_{\mathbf{x}} \ell(y, \mathbf{x}, \mathbf{w}). \quad (13)$$

It is not difficult to see that, for any given point \mathbf{x} , y , the optimization problem for evasion attacks in Eqs. (2)-(3) (without considering the feature bounds in Eq. 4) can be rewritten as:

$$\hat{\boldsymbol{\delta}} \in \arg \max_{\|\boldsymbol{\delta}\|_p \leq \varepsilon} \ell(y, \mathbf{x} + \boldsymbol{\delta}, \hat{\mathbf{w}}). \quad (14)$$

Under the same linear approximation, this corresponds to the maximization of an inner product over an ε -sized ball:

$$\max_{\|\boldsymbol{\delta}\|_p \leq \varepsilon} \boldsymbol{\delta}^\top \nabla_{\mathbf{x}} \ell(y, \mathbf{x}, \hat{\mathbf{w}}) = \varepsilon \|\nabla_{\mathbf{x}} \ell(y, \mathbf{x}, \hat{\mathbf{w}})\|_q, \quad (15)$$

where ℓ_q is the dual norm of ℓ_p .

The above problem is maximized as follows:

- (1) For $p = 2$, the maximum is $\hat{\delta} = \varepsilon \frac{\nabla_{\mathbf{x}} \ell(y, \mathbf{x}, \hat{\mathbf{w}})}{\|\nabla_{\mathbf{x}} \ell(y, \mathbf{x}, \hat{\mathbf{w}})\|_2}$;
- (2) For $p = \infty$, the maximum is $\hat{\delta} \in \varepsilon \cdot \text{sign}\{\nabla_{\mathbf{x}} \ell(y, \mathbf{x}, \hat{\mathbf{w}})\}$;
- (3) For $p = 1$, the maximum is achieved by setting the values of $\hat{\delta}$ that correspond to the maximum absolute values of $\nabla_{\mathbf{x}} \ell(y, \mathbf{x}, \hat{\mathbf{w}})$ to their sign, i.e., ± 1 , and 0 otherwise.

Substituting the optimal value of $\hat{\delta}$ into Eq. (13), we can compute the increase of the loss function $\Delta \ell = \hat{\delta}^\top \nabla_{\mathbf{x}} \ell(y, \mathbf{x}, \mathbf{w})$ under a transfer attack in closed form. For example, for $p = 2$, it is given as:

$$\Delta \ell = \varepsilon \frac{\nabla_{\mathbf{x}} \hat{\ell}^\top}{\|\nabla_{\mathbf{x}} \hat{\ell}\|_2} \nabla_{\mathbf{x}} \ell \leq \varepsilon \|\nabla_{\mathbf{x}} \ell\|_2, \quad (16)$$

where, for compactness, we use $\hat{\ell} = \ell(y, \mathbf{x}, \hat{\mathbf{w}})$ and $\ell = \ell(y, \mathbf{x}, \mathbf{w})$. In this equation, the left-hand side is the increase in the loss function in the black-box case, while the right-hand side corresponds to the white-box case. The upper bound is obtained when the surrogate classifier $\hat{\mathbf{w}}$ is equal to the target \mathbf{w} (white-box attacks). Similar results hold for $p = 1$ and $p = \infty$ (using the dual norm in the right-hand side).

Intriguing Connections and Transferability Metrics.. The above findings reveal some interesting connections among transferability of attacks, regularization and size of input gradients, as detailed below, and allow us to define simple and computationally-efficient transferability metrics.

(1) *Size of Input Gradients.* The first interesting observation is that transferability depends on the size of the gradient of the loss ℓ computed using the *target* classifier, regardless of the surrogate: the larger this gradient is, the larger the attack impact may be. This is inferred from the upper bound in Eq. (16). We define the corresponding metric $S(\mathbf{x}, y)$ as:

$$S(\mathbf{x}, y) = \|\nabla_{\mathbf{x}} \ell(y, \mathbf{x}, \mathbf{w})\|_q, \quad (17)$$

where q is the dual of the perturbation norm.

The size of the input gradient also depends on the complexity of the model, given, for instance, by its level of regularization. Less complex, highly-regularized classifiers tend to have smaller input gradients, i.e., they learn smoother functions that are more robust to attacks, and vice-versa. Notably, this holds for both evasion and poisoning attacks (e.g., the poisoning gradient in Eq. (10) is proportional to α_c , which is larger when the model is weakly regularized). This result has also another interesting consequence: if a classifier has large input gradients (e.g., due to high-dimensionality of the input space and low level of regularization), for an attack to succeed it suffices to apply only tiny, *imperceptible* perturbations. As we will see in the experimental section, this explains why adversarial examples against deep neural networks can often only be slightly perturbed to mislead detection, while when attacking less complex classifiers in low dimensions, modifications become more evident.

(2) *Gradient Alignment.* The second relevant impact factor on transferability is based on the alignment of the input gradients of the loss function computed using the target and the surrogate learners. If we compare the increase in the loss function in the black-box case (the left-hand side of Eq. 16) against that corresponding to white-box attacks (the right-hand side), we find that the relative increase

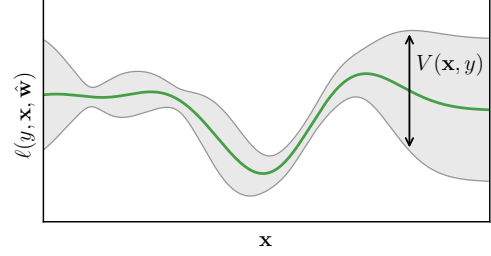


Figure 3: Conceptual representation of the variability of the loss landscape. The green line represents the expected loss with respect to different training sets used to learn the surrogate model, while the gray area represents the variance of the loss landscape. If the variance is too large, local optima may change, and the attack may not successfully transfer.

in loss, at least for ℓ_2 perturbations, is given by the following value:

$$R(\mathbf{x}, y) = \frac{\nabla_{\mathbf{x}} \hat{\ell}^\top \nabla_{\mathbf{x}} \ell}{\|\nabla_{\mathbf{x}} \hat{\ell}\|_2 \|\nabla_{\mathbf{x}} \ell\|_2}. \quad (18)$$

Interestingly, this is exactly the cosine of the angle between the gradient of the loss of the surrogate and that of the target classifier. This is a novel finding which explains why the cosine angle metric between the target and surrogate gradients can well characterize the transferability of attacks. Worth noting, for other kinds of perturbation, this definition slightly changes, but gradient alignment can be similarly evaluated.

(3) *Variability of the Loss Landscape.* We define here another useful metric to characterize attack transferability. The idea is to measure the variability of the loss function $\hat{\ell}$ when the training set used to learn the surrogate model changes, even though it is sampled from the same underlying distribution. The reason is that the loss $\hat{\ell}$ is exactly the objective function \mathcal{A} optimized by the attacker to craft evasion attacks (Eq. 1). Accordingly, if this loss landscape changes dramatically even when simply resampling the surrogate training set (which may happen, e.g., for surrogate models exhibiting a large error variance, like neural networks and decision trees), it is very likely that the local optima of the corresponding optimization problem will change, and this may in turn imply that the attacks will not transfer correctly to the target learner.

We define the variability of the loss landscape simply as the *variance* of the loss, estimated at a given attack point \mathbf{x}, y :

$$V(\mathbf{x}, y) = \mathbb{E}_{\mathcal{D}} \{\ell(y, \mathbf{x}, \hat{\mathbf{w}})^2\} - \mathbb{E}_{\mathcal{D}} \{\ell(y, \mathbf{x}, \hat{\mathbf{w}})\}^2, \quad (19)$$

where $\mathbb{E}_{\mathcal{D}}$ is the expectation taken with respect to different (surrogate) training sets. This is very similar to what is typically done to estimate the variance of classifiers' predictions. This notion is clarified also in Fig. 3.

The transferability metrics S , R and V defined so far depend on the initial attack point \mathbf{x} and its label y . In our experiments, we will compute their mean values by averaging on different initial attack points.

Transferability of Poisoning Attacks.. For poisoning attacks, we can essentially follow the same derivation discussed before. Instead of defining transferability in terms of the loss attained on

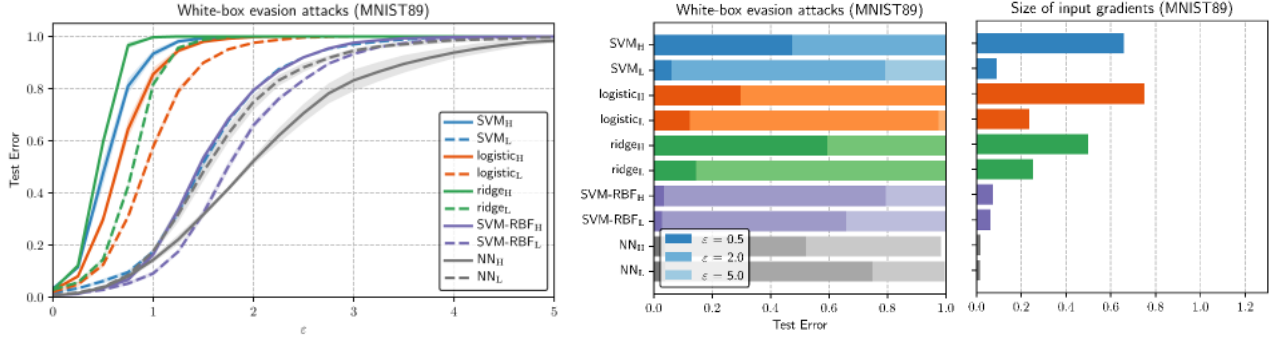


Figure 4: White-box evasion attacks on MNIST89. Test error as a function of the maximum perturbation $\epsilon \in [0, 5]$ (left). Test error for 3 levels of perturbation: $\epsilon \in \{0.5, 2, 5\}$ (middle). Average size of input gradients S (Eq. 17) for target classifiers (right).

the modified test point, we define it in terms of the validation loss attained by the target classifier under the influence of the poisoning points. This loss function can be linearized as done in the previous case, yielding: $T \approx L(\mathcal{D}, \mathbf{w}) + \hat{\delta}^\top \nabla_{\mathbf{x}} L(\mathcal{D}, \mathbf{w})$, where \mathcal{D} are the untainted validation points, and $\hat{\delta}$ is the perturbation applied to the initial poisoning point \mathbf{x} against the surrogate classifier. Recall that L depends on the poisoning point through the classifier parameters \mathbf{w} , and that the gradient $\nabla_{\mathbf{x}} L(\mathcal{D}, \mathbf{w})$ here is equivalent to the generic one reported in Eq. (9). It is then clear that the perturbation $\hat{\delta}$ maximizes the (linearized) loss when it is best aligned with its derivative $\nabla_{\mathbf{x}} L(\mathcal{D}, \mathbf{w})$, according to the constraint used, as in the previous case. The three transferability metrics defined before can also be used for poisoning attacks provided that we simply replace the evasion loss $\ell(y, \mathbf{x}, \mathbf{w})$ with the validation loss $L(\mathcal{D}, \mathbf{w})$.

5 EXPERIMENTAL ANALYSIS

In this section, we evaluate the transferability of both evasion and poisoning attacks across a range of ML models. We highlight some interesting findings about transferability, based on the three metrics developed in Sect. 4. In particular, we analyze attack transferability in terms of its connection to the size of the input gradients of the loss function, the gradient alignment between surrogate and target classifiers, and the variability of the loss function optimized to craft the attack points. We provide recommendations on how to choose the most effective surrogate models to craft transferable attacks in the black-box setting.

5.1 Transferability of Evasion Attacks

We start by reporting our experiments on evasion attacks. We consider here two distinct case studies, involving handwritten digit recognition and Android malware detection.

5.1.1 Handwritten Digit Recognition. The MNIST89 data includes the MNIST handwritten digits from classes 8 and 9. Each digit image consists of 784 pixels ranging from 0 to 255, normalized in $[0, 1]$ by dividing such values by 255. We run 5 independent repetitions to average the results on different training-test splits. In each repetition, we run white-box and black-box attacks, using 3,000 samples to train the target classifier and 1,000 distinct samples to train the surrogate classifier (without even relabeling the surrogate data with labels predicted by the target classifier; i.e., we do not perform any

query on the target). We modified test digits in both classes using an ℓ_2 -constrained attack with $\epsilon \in [0, 5]$.

We consider the following classifiers from scikit-learn [32]: (i) SVMs with linear kernel (SVM_H with $C = 100$ and SVM_L with $C = 0.01$); (ii) SVMs with RBF kernel (SVM-RBF_H with $C = 100$ and SVM-RBF_L with $C = 1$, both with $\gamma = 0.01$); (iii) logistic classifiers (logistic_H with $C = 10$ and logistic_L with $C = 1$); (iv) ridge classifiers (ridge_H with $\alpha = 1$ and ridge_L with $\alpha = 10$); (v) fully-connected neural networks with two hidden layers and ReLU as activation function (NN_H with 200 hidden neurons and NN_L with 50 hidden neurons); and (vi) random forests (RF_H with no limit on the number of trees and RF_L with a max depth of 8 trees). These configurations are chosen to evaluate the robustness of classifiers that exhibit similar test accuracies but different levels of regularization. We use subscripts *H* and *L* to denote high-complexity and low-complexity models, respectively.¹

How does model complexity impact evasion attack success in the white-box setting? The results for white-box evasion attacks are reported in Fig. 4 for all classifiers that fall under our framework and can be tested for evasion with gradient-based optimization attacks (SVM, Logistic, Ridge, and Neural Networks). This excludes random forests, as they are not differentiable. We report the complete *security evaluation curves* on the left, showing the mean test error (over 5 runs) against an increasing maximum admissible distortion ϵ . The results clearly show that *less complex* (i.e., *strongly regularized*) classifiers are *less vulnerable to evasion attacks*. The underlying reason is that classifier vulnerability depends on model complexity (via the size of the input gradients), which is in turn reduced when classification functions are smoother and more regularized.

In the middle graph in Fig. 4 we show the test error for three levels of perturbation ($\epsilon \in \{0.5, 2, 5\}$), and on the right the size of the input gradients of the loss computed on the target classifier. We observe that models with larger gradient norms are easier to attack in the white-box setting, confirming our theoretical analysis. Moreover, we observe that for each family of classifiers, lower regularization results in larger input gradients and higher test error. This validates the correlation between model resilience to evasion attack and gradient norms. This holds for both linear (e.g., SVM

¹Recall that the level of regularization increases as α increases, and as C decreases.

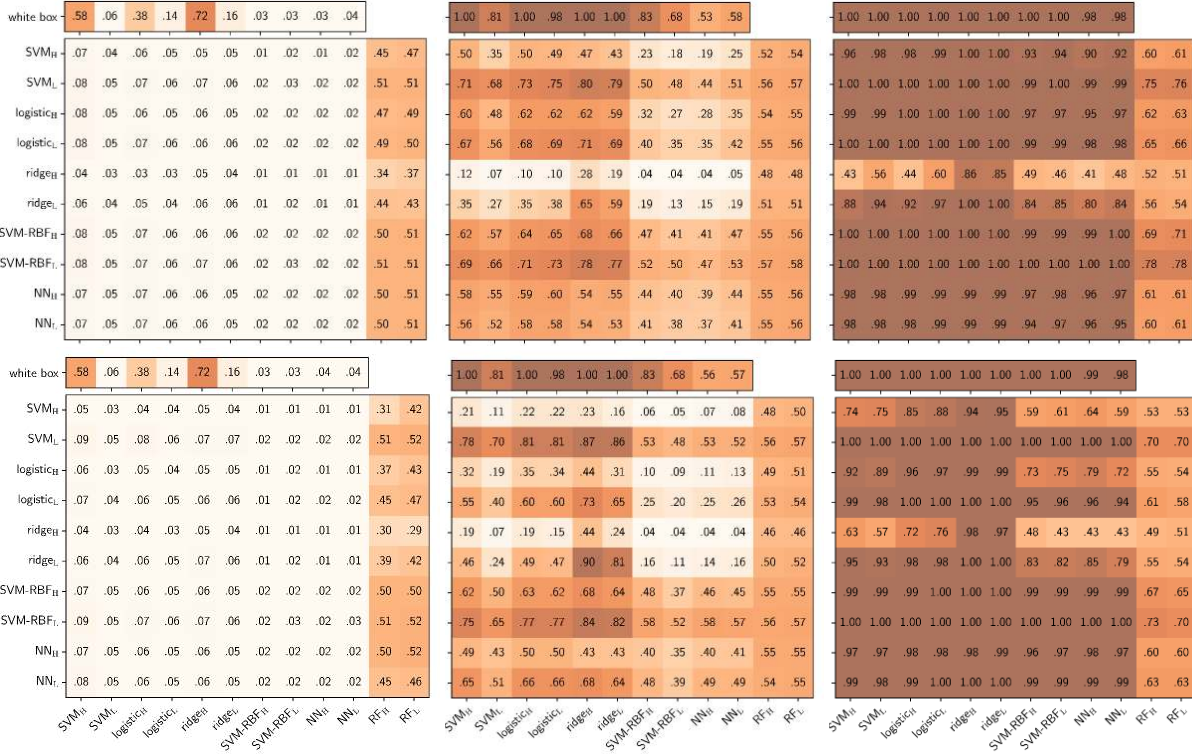


Figure 5: Transferability of black-box evasion results on MNIST. Each cell in a matrix contains the test error of the target classifiers (in columns) on the attack samples crafted against the surrogate learners (in rows). Top row uses 20% training data, while bottom row uses 100% training data for surrogate model. The columns show test errors for different values of ϵ (0.5 left, 2 middle, and 5 right). Darker color means higher test error and indicates higher transferability.

with linear kernel, ridge, and logistic regression) and non-linear classifiers (e.g., SVM-RBF). Another interesting finding is that non-linear classifiers tend to be in general less vulnerable than linear ones.

How do evasion attacks transfer between models in black-box settings? In Fig. 5 we report test error for transferability across all models that can be attacked in white-box setting (rows in the matrix) and all considered targeted models (columns in the matrix). The top row shows results for using a subset (20%) of training data in the surrogate model, while the bottom row shows results for all training data in the surrogate model. The three columns represent the results for three levels of perturbation ($\epsilon = 0.5$ on the left, $\epsilon = 2$ in the middle, and $\epsilon = 5$ on the right).

It can be noted that lower-complexity models (with stronger regularization) provide better surrogate models, on average. In particular, this can be seen best in the middle column for medium level of perturbation, in which the lower-complexity models (SVM_L, logistic_L, ridge_L, and SVM-RBF_L) provide on average higher error when transferred to other models. The reason is that they learn smoother and stabler functions, that are capable of better approximating the target function. Surprisingly, this holds also when using only 20% of training data (top row in Fig. 5), as the black-box attacks relying on such low-complexity models still transfer with similar test errors. This means that most classifiers can be attacked in this

black-box setting with almost no knowledge of the model, no query access, but provided that one can get a small amount of data similar to that used to train the target model.

These findings are also confirmed by looking at the variability of the loss landscape, computed as discussed in Sect. 4 (by considering 5 different training sets), and reported in Fig. 7. It is clear here too that higher-variance classifiers are less effective as surrogate than their less-complex counterparts, as the former tend to provide worse, unstable approximations of the target classifier.

Another interesting, related observation is that the adversarial examples computed against lower-complexity surrogates have to be perturbed more to evade (see Fig. 8), whereas the perturbation of the ones computed against complex models can be smaller. This is again due to the instability induced by high-complexity models into the loss function optimized to craft evasion attacks, whose sudden changes cause the presence of closer local optima to the initial attack point.

On the vulnerability of random forests. A noteworthy finding is that random forests can be effectively attacked at small perturbation levels using most other models (see last two columns in Fig. 5). We looked at the learned trees and discovered that trees often are susceptible to small changes. In one example, a node of the tree checked if a particular feature value was above 0.002, and classified samples as digit 8 if that condition holds (and digit 9 otherwise).

The attack modified that feature from value 0 to 0.028, causing it to be immediately misclassified. This vulnerability is intrinsic in the selection process of the threshold values used by these decision trees to split each node. The threshold values are selected among the existing values in the dataset (to correctly handle categorical attributes). Therefore, for pixels which are highly discriminant (e.g., mostly black for one class and white for the other), the threshold will be either very close to one extreme or the other, making it easy to subvert the prediction by a small change. Since ℓ_2 -norm attacks change almost all feature values, with high probability the attack modifies at least one feature on every path of the tree, causing misclassification.

Is gradient alignment an effective transferability metric? In Fig. 6, we show on the right the Pearson correlation between perturbations generated with different models, while we show on the left the alignment between the input gradients of the surrogate (in rows) and of the target model (in columns). We observe immediately that the cosine angle provides an accurate measure of transferability: the higher the cosine angle, the higher the correlation (meaning that the adversarial examples for the two models are similar). Worth remarking, this measure is extremely fast to evaluate, as it does not require simulating any attack. Nevertheless, this is only a relative measure of the attack transferability, as its final impact depends on how much the target classifier is regularized; i.e., on the size of the input gradients of the target classifier.

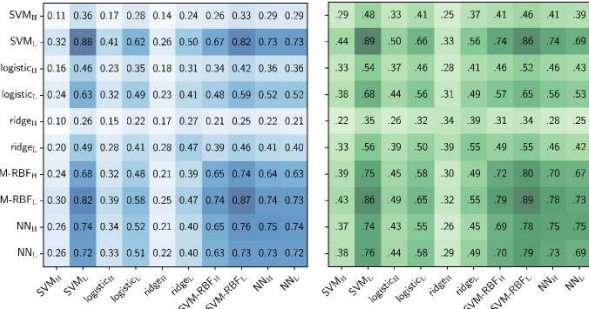


Figure 6: Gradient alignment R (Eq. 18) between surrogate (in rows) and target (in columns) classifiers, averaged on the unmodified test samples (left). Pearson correlation between perturbations on the MNIST89 dataset for evasion (right).

5.1.2 Android Malware Detection. The Drebin data [1] consists of around 120,000 legitimate and around 5000 malicious Android applications, labeled using the VirusTotal service. A sample is labeled as malicious (or positive, $y = +1$) if it is classified as such from at least five out of ten anti-virus scanners, while it is flagged as legitimate (or negative, $y = -1$) otherwise. The structure and the source code of each application is encoded as a *sparse* feature vector consisting of around a million binary features denoting the presence or absence of permissions, suspicious URLs and other relevant information that can be extracted by statically analyzing Android applications. Since we are working with sparse binary features, we use the ℓ_1 norm for the attack.

We use 30,000 samples to learn surrogate and target classifiers, and 30,000 samples for testing. The configurations of classifiers is

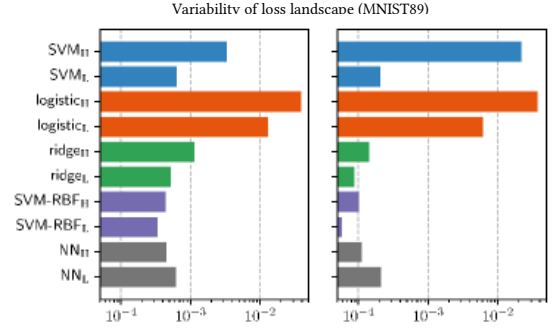


Figure 7: Variability V (Eq. 19) of the loss of the surrogate learner trained on MNIST89, with 20% (left) and 100% (right) training samples, averaged on the unmodified test samples.

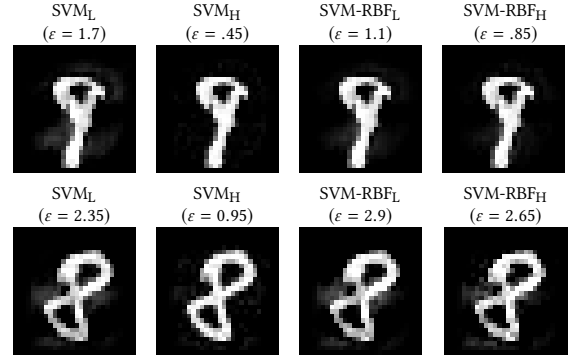


Figure 8: Digit images crafted to evade linear and RBF SVMs. The values of ϵ reported here correspond to the minimum perturbation required to evade detection. Larger perturbations are required to mislead low-complexity classifiers (L), while smaller ones suffice to evade high-complexity classifiers (H).

the same used for MNIST89, apart from (i) the number of hidden neurons of the fully-connected NNs (NN_H with 800 hidden neurons and NN_L with 200 hidden neurons); and (ii) the random forest classifiers (RF_H with no limit on the number of trees and RF_L with a max depth of 59 trees).

We perform feature selection to retain those 5,000 features which maximize information gain, i.e., $|p(x_k = 1|y = +1) - p(x_k = 1|y = -1)|$, where x_k is the k^{th} feature. While this feature selection process does not significantly affect the detection rate (which is only reduced by 2%, on average, at 1% false alarm rate), it drastically reduces the computational complexity of classification.

In each experiment, we run white-box and black-box evasion attacks on 1,000 distinct malware samples (randomly selected from the test data) against an increasing number of modified features in each malware $\epsilon \in \{0, 1, 2, \dots, 30\}$. This is achieved by imposing the ℓ_1 constraint $\|\mathbf{x}' - \mathbf{x}\|_1 \leq \epsilon$. As in previous work, we further restrict the attacker to only *inject* features into each malware sample, to avoid compromising its intrusive functionality [3, 10].

To evaluate the impact of the aforementioned evasion attack, we measure the evasion rate (i.e., the fraction of malware samples misclassified as legitimate) at 1% false alarm rate (i.e., when only 1%

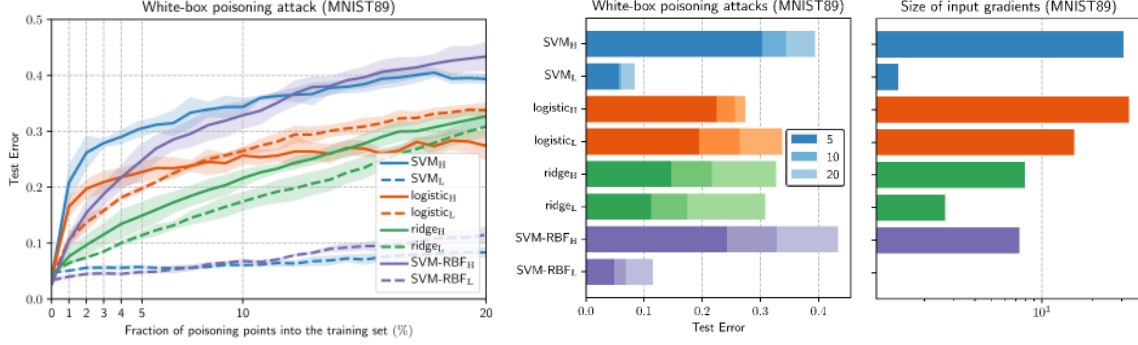


Figure 9: White-box poisoning attacks on MNIST89. Test error as a function of the percentage of poisoning points $\varepsilon \in [5\%, 20\%]$ (left). Test error for three levels of poisoning rates: $\varepsilon \in 5, 10, 20\%$ (middle). Average size of input gradients S (Eq. 17) for target classifiers (right).

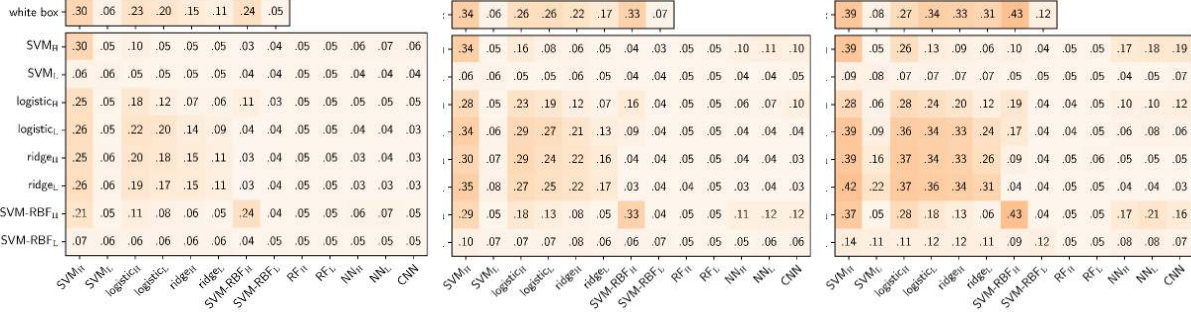


Figure 10: Transferability of black-box poisoning attacks on MNIST89. We report error for different percentages of poisoning (5% on left, 10% in the middle, and 20% on the right). The surrogate models are in the rows and the target models in the columns. Darker color means higher test error and indicates higher transferability.

of the legitimate samples are misclassified as malware). As in the previous experiment, we report the complete *security evaluation curve* for the white-box attack case, whereas we report only the value of test error for the black-box case. The results, reported in Fig. 14 (white-box evasion results), Fig. 15 (black-box transferability results), Fig. 16 (gradient alignment), and Fig. 17 (loss variance) in Appendix 8.1, confirm the main findings of the previous experiments. One significant difference is that random forests are much more robust in this case. The reason is that the ℓ_1 -norm attack (differently from the ℓ_2) only changes a small number of features, and thus the probability that it will change features in all the ensemble trees is very low.

5.2 Transferability of Poisoning Attacks

For poisoning attacks, we report experiments on handwritten digits and face recognition.

5.2.1 Handwritten Digit Recognition. We apply our optimization framework to poison SVM, logistic, and ridge classifiers in the white-box setting. Designing efficient poisoning availability attacks against neural networks is still an open problem due to the high complexity of the bilevel optimization and the non-convexity of the decision boundary. Previous work has mainly considered targeted poisoning attacks against neural networks [18, 40], and it is

believed that neural networks are much more resilient to poisoning availability attacks due to their memorization capability. Poisoning random forests is not feasible with gradient-based attacks, and we are not aware of any existing attacks for this ensemble method. We thus consider as surrogate learners: (i) linear SVMs with $C = 0.01$ (SVM_L) and $C = 100$ (SVM_H); (ii) logistic classifiers with $C = 1$ ($logistic_L$) and $C = 10$ ($logistic_H$); (iii) ridge classifiers with $\alpha = 100$ ($ridge_L$) and $\alpha = 10$ ($ridge_H$); and (iv) SVMs with RBF kernel with $\gamma = 0.01$ and $C = 1$ ($SVM-RBF_L$) and $C = 100$ ($SVM-RBF_H$). We additionally consider as target classifiers: (i) random forests with a number of base trees equal to 6 for RF_L and 15 for RF_H ; (ii) feed-forward neural networks with a single hidden layer consisting of 50 (NN_L) or 200 (NN_H) neurons; and (iii) a Convolutional Neural Network (CNN) using the same architecture as in [6].

We consider 500 training samples, 1,000 validation samples to compute the attack, and a separate set of 1,000 test samples to evaluate the error. The test error is computed against an increasing number of poisoning points into the training set, from 0% to 20% (corresponding to 125 poisoning points). The reported results are averaged on 5 independent, randomly-drawn data splits.

How does model complexity impact poisoning attack success in the white-box setting? The results for white-box poisoning are reported in Fig. 9. Similarly to the evasion case, more complex classifiers are more vulnerable to poisoning attacks. In the

middle graph in Fig. 9 we show the test error for three levels of poisoning (5%, 10%, and 20%), and on the right the size of the input gradients for the target classifiers. We confirm that the poisoning gradients are larger for more complex (e.g., weakly regularized) models, and the resilience of models against poisoning attacks is highly correlated to their gradient size. Therefore, model complexity plays a large role in a model’s robustness against poisoning attacks, confirming our analysis.

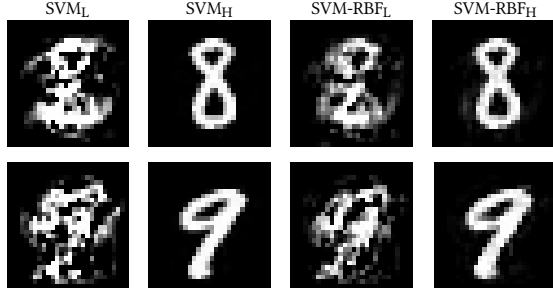


Figure 11: Poisoning digits crafted against linear and RBF SVMs. Larger perturbations are required to have significant impact on low-complexity classifiers (L), while minimal changes are very effective on high-complexity SVMs (H).

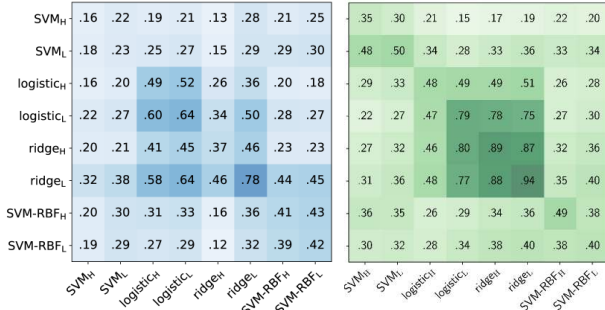


Figure 12: Gradient alignment R (Eq. 18) between surrogate (in rows) and target (in columns) classifiers, averaged on the unmodified test samples (left). Pearson correlation between perturbations on the MNIST89 dataset for evasion (right).

How do poisoning attacks transfer between models in black-box settings? The results for black-box poisoning are reported in Fig. 10. For poisoning attacks, the best surrogate classifiers are those matching the complexity of the target (for instance, models with same regularization level). This is different from evasion attacks, which seem to transfer better from low-complexity models. The reason is that, in the case of poisoning, the loss landscape optimized by the attacker is anyway much stabler than in the case of evasion. This is well demonstrated if one considers the variance of the loss function optimized for poisoning attacks in Fig. 13. In fact, these mean variance values are much smaller than those reported in the evasion case (on the order of 10^{-5}). The reason is that, while the evasion loss ℓ is computed on the single evasion point, the poisoning loss L is computed as the average loss on the validation points, and

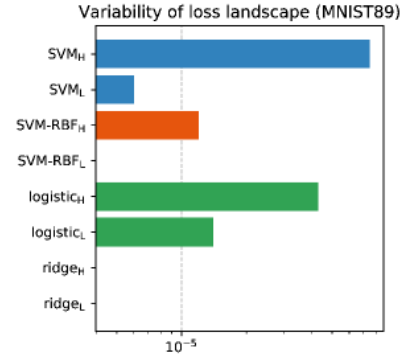


Figure 13: Variability V (Eq. 19) of the loss of the surrogate learner on MNIST89, averaged on different poisoning points.

this averaging process significantly reduces the variance of the objective function. This explains why, even for high-complexity models, poisoning attacks can transfer successfully. This is also confirmed by the alignment of the loss gradients reported in Fig. 12. A visual inspection of the poisoning digits, shown in Fig. 11, reveals that the poisoning points crafted against high-complexity classifiers are only minimally perturbed, while the ones computed against low-complexity classifiers exhibit larger, visible perturbations. This is again due to the presence of closer local optima in the former case.

5.2.2 Face Recognition. The Labeled Face on the Wild (LFW) dataset consists of faces of famous peoples collected on Internet. We considered the six identities with the largest number of images in the dataset. We considered the person with most images as positive class, and all the others as negative. Our dataset consists of 530 positive and 758 negative images. The results are shown in Appendix 8.2 (Fig. 18 for white-box poisoning results, Fig. 19 for transferability of black-box attacks, Fig. 20 for the correlation and cosine angle between gradients, and Fig. 22 for examples of perturbed faces at different levels of regularization), confirming the same insights.

5.3 Summary of Transferability Evaluation

We summarize the results of transferability for evasion and poisoning attacks below:

- (1) Lower complexity (for instance, strongly-regularized) classifiers are less vulnerable to evasion and poisoning attacks due to the size of their input gradients. In general, non-linear models are more robust than linear models to both types of attacks.
- (2) The gradient alignment between surrogate and target classifiers provides a reliable metric to identify good surrogate models and evaluate transferability.
- (3) Lower variance of the optimization objective used by the attacker results in better transferability.
- (4) Models with lower complexity and lower variance often provide adversarial examples that transfer better to a range of models for evasion attacks. For poisoning attacks, the best surrogates are generally models with similar levels of

regularization as the target model. The reason is that the poisoning objective function is relatively stable (i.e., has low variance) for most classifiers, and the gradient alignment between the surrogate and target classifiers becomes a more important factor.

Our recommendation to performing evasion attacks in the realistic black-box attack model is to choose surrogate classifiers with relatively low level of complexity (e.g., by using strong regularization and reducing model variance). To perform poisoning attacks, our recommendation is to acquire additional information about the level of regularization of the target and use surrogate model with the same level of regularization as the target classifier.

We highlight that lower complexity classifiers are more resilient to both evasion and poisoning attacks. Therefore, we recommend classifier designers to favor low-complexity models, when there is a risk of malicious threat. Of course, we need to take into account the bias-variance trade-off and choose models that still perform relatively well on the original prediction tasks (and do not underfit to the training data).

6 RELATED WORK

Transferability for evasion attacks.. Transferability of evasion attacks has been studied in previous work, e.g., [3, 12, 13, 19, 24, 30, 31, 41, 42, 45].

Goodfellow et al. [13], Tramer et al. [42], and Moosavi et al. [24] make the observation that different models might learn intersecting decision boundaries in both benign and adversarial dimensions and in that case adversarial examples transfer better. Tramer et al. also perform a detailed study of transferability of model-agnostic perturbations that depend only on the training data (using also MNIST and Drebin). They notice that adversarial examples crafted against linear models transfer to higher-order models. We answer some of the open questions they posed about factors contributing to attack transferability. Liu et al. [19] have empirically observed the gradient alignment between models with transferable adversarial examples. Papernot et al. [30, 31] observe that adversarial examples transfer across a range of models, including logistic regression, decision trees, SVMs, and neural networks, but do not provide an explanation of the phenomena.

Prior work has investigated the role of input gradients and Jacobians. Some of these works have considered training in order to decrease the magnitude of input gradients to defend against evasion attacks [20, 34] or improve classification accuracy [39, 43]. In [38], the magnitude of the input gradient is identified as a cause for vulnerability to evasion attacks.

A number of papers (e.g., [12, 19, 45]) have shown that transferability of adversarial examples is increased by averaging the gradients computed for ensembles of models. We highlight that we obtain similar effect by attacking a strongly-regularized surrogate model with smoother and more stable decision boundary (resulting in a lower-variance model). The advantage of our approach is to reduce the computational complexity compared to attacking classifier ensembles.

Through our formalization of transferability, we shed light on the most important factors for transferability. In particular, we identify a set of conditions that explain transferability including

the gradient alignment between the surrogate and targeted models, and the size of the input gradients of the target model, connected to model complexity. We demonstrate that adversarial examples crafted against lower-variance models (e.g., those that are strongly regularized) tend to transfer better across a range of models.

Transferability for poisoning attacks.. In the context of poisoning availability attacks there is very little work on transferability, the exception being a preliminary investigation [25]. That work indicates that poisoning examples are transferable among very simple network architectures (logistic regression, MLP, and Adaline). Transferability of targeted poisoning attacks has been addressed recently in [40]. We are the first to study in depth transferability of poisoning availability attacks.

7 CONCLUSIONS

We conducted an analysis and experimental evaluation of the transferability of evasion and poisoning attacks under a unified optimization framework. Our theoretical transferability formalization sheds light on various factors impacting the transfer success rates. In particular, we define three metrics that impact the transferability of an attack, including the complexity of the target model, the gradient alignment between the surrogate and target models, and the variance of the attacker optimization objective. The lesson to system designers is to evaluate their classifiers against these criteria and select lower-complexity, stronger regularized models that tend to provide higher robustness to both evasion and poisoning.

Interesting avenues for future work are extending our analysis to multi-class classification settings, and considering a range of gray-box models in which attackers might have additional knowledge on the machine learning system (as in [40]). Application-dependent scenarios such as cyber security might provide additional constraints on threat models and attack scenarios and could impact transferability in interesting ways.

REFERENCES

- [1] D. Arp, M. Spreitzerbarth, M. Hübner, H. Gascon, and K. Rieck. 2014. Drebin: Efficient and explainable detection of android malware in your pocket. In *Proc. 21st Annual Network & Distributed System Security Symposium (NDSS)*. The Internet Society.
- [2] A. Athalye, N. Carlini, and D. Wagner. 2018. Obfuscated Gradients Give a False Sense of Security: Circumventing Defenses to Adversarial Examples. *ArXiv e-prints* (2018).
- [3] B. Biggio, I. Corona, D. Maiorca, B. Nelson, N. Šrndić, P. Laskov, G. Giacinto, and F. Roli. 2013. Evasion attacks against machine learning at test time. In *Machine Learning and Knowledge Discovery in Databases (ECML PKDD), Part III (LNCS)*, Hendrik Blockeel, Kristian Kersting, Siegfried Nijssen, and Filip Železný (Eds.), Vol. 8190. Springer Berlin Heidelberg, 387–402.
- [4] Battista Biggio, Blaine Nelson, and Pavel Laskov. 2012. Poisoning attacks against support vector machines. In *29th Int'l Conf. on Machine Learning*, John Langford and Joelle Pineau (Eds.), *Int'l Conf. on Machine Learning (ICML)*, 1807–1814.
- [5] B. Biggio and F. Roli. 2018. Wild Patterns: Ten Years After the Rise of Adversarial Machine Learning. *ArXiv e-prints* (2018).
- [6] Nicholas Carlini and David A. Wagner. 2017. Adversarial Examples Are Not Easily Detected: Bypassing Ten Detection Methods. In *10th ACM Workshop on Artificial Intelligence and Security (AISec '17)*, Bhavani M. Thuraisingham, Battista Biggio, David Mandell Freeman, Brad Miller, and Arunesh Sinha (Eds.). ACM, New York, NY, USA, 3–14.
- [7] Nicholas Carlini and David A. Wagner. 2017. Towards Evaluating the Robustness of Neural Networks. In *IEEE Symposium on Security and Privacy*. IEEE Computer Society, 39–57.
- [8] X. Chen, C. Liu, B. Li, K. Lu, and D. Song. 2017. Targeted Backdoor Attacks on Deep Learning Systems Using Data Poisoning. *ArXiv e-prints* abs/1712.05526 (2017).

- [9] Hung Dang, Yue Huang, and Ee-Chien Chang. 2017. Evading Classifiers by Morphing in the Dark. In *Proceedings of the 24th ACM SIGSAC Conference on Computer and Communications Security (CCS)*.
- [10] Ambra Demontis, Marco Melis, Battista Biggio, Davide Maiorca, Daniel Arp, Konrad Rieck, Igino Corona, Giorgio Giacinto, and Fabio Roli. In press. Yes, Machine Learning Can Be More Secure! A Case Study on Android Malware Detection. *IEEE Trans. Dependable and Secure Computing* (In press).
- [11] Ambra Demontis, Paolo Russu, Battista Biggio, Giorgio Fumera, and Fabio Roli. 2016. On Security and Sparsity of Linear Classifiers for Adversarial Settings. In *Joint IAPR Int'l Workshop on Structural, Syntactic, and Statistical Pattern Recognition (LNC3)*, Antonio Robles-Kelly, Marco Loog, Battista Biggio, Francisco Escolano, and Richard Wilson (Eds.), Vol. 10029. Springer International Publishing, Cham, 322–332.
- [12] Yinpeng Dong, Fangzhou Liao, Tianyu Pang, Hang Su, Jun Zhu, Xiaolin Hu, and Jianguo Li. 2018. Boosting Adversarial Examples with Momentum. In *CVPR*.
- [13] Ian J. Goodfellow, Jonathon Shlens, and Christian Szegedy. 2015. Explaining and Harnessing Adversarial Examples. In *International Conference on Learning Representations*.
- [14] Kathrin Grosse, Nicolas Papernot, Praveen Manoharan, Michael Backes, and Patrick D. McDaniel. 2017. Adversarial Examples for Malware Detection. In *ESORICS (2) (LNC3)*, Vol. 10493. Springer, 62–79.
- [15] Tianyu Gu, Brendan Dolan-Gavitt, and Siddharth Garg. 2017. BadNets: Identifying Vulnerabilities in the Machine Learning Model Supply Chain. In *NIPS Workshop on Machine Learning and Computer Security*, Vol. abs/1708.06733.
- [16] M. Jagielski, A. Oprea, B. Biggio, C. Liu, C. Nita-Rotaru, and B. Li. 2018. Manipulating Machine Learning: Poisoning Attacks and Countermeasures for Regression Learning. In *IEEE Symposium on Security and Privacy (SP '18)*. IEEE CS, 931–947. <https://doi.org/10.1109/SP.2018.00057>
- [17] Alex Kantchelian, J. D. Tygar, and Anthony D. Joseph. 2016. Evasion and Hardening of Tree Ensemble Classifiers. In *33rd ICML (JMLR Workshop and Conference Proceedings)*, Vol. 48. JMLR.org, 2387–2396.
- [18] Pang Wei Koh and Percy Liang. 2017. Understanding black-box predictions via influence functions. In *Proc. 34th International Conference on Machine Learning (ICML)*.
- [19] Yanpei Liu, Xinyun Chen, Chang Liu, and Dawn Song. 2017. Delving into Transferable Adversarial Examples and Black-box Attacks. In *ICLR*.
- [20] Chunchuan Lyu, Kaizhu Huang, and Hai-Ning Liang. 2015. A Unified Gradient Regularization Family for Adversarial Examples. In *2015 IEEE International Conference on Data Mining (ICDM)*, Vol. 00. IEEE Computer Society, Los Alamitos, CA, USA, 301–309.
- [21] A. Madry, A. Makelov, L. Schmidt, D. Tsipras, and A. Vladu. 2018. Towards Deep Learning Models Resistant to Adversarial Attacks. In *ICLR*.
- [22] Shike Mei and Xiaojin Zhu. 2015. Using Machine Teaching to Identify Optimal Training-Set Attacks on Machine Learners. In *29th AAAI Conf. Artificial Intelligence (AAAI '15)*.
- [23] Marco Melis, Ambra Demontis, Battista Biggio, Gavin Brown, Giorgio Fumera, and Fabio Roli. 2017. Is Deep Learning Safe for Robot Vision? Adversarial Examples against the iCub Humanoid. In *ICCVW Vision in Practice on Autonomous Robots (ViPAR)*. IEEE, 751–759.
- [24] Seyed-Mohsen Moosavi-Dezfooli, Alhussein Fawzi, Omar Fawzi, and Pascal Frossard. 2017. Universal adversarial perturbations. In *CVPR*.
- [25] Luis Muñoz-González, Battista Biggio, Ambra Demontis, Andrea Paudice, Vasin Wongrassamee, Emil C. Lupu, and Fabio Roli. 2017. Towards Poisoning of Deep Learning Algorithms with Back-gradient Optimization. In *10th ACM Workshop on Artificial Intelligence and Security (AISec '17)*, Bhavani M. Thuraisingham, Battista Biggio, David Mandell Freeman, Brad Miller, and Arunesh Sinha (Eds.). ACM, New York, NY, USA, 27–38.
- [26] Blaine Nelson, Marco Barreno, Fuchang Jack Chi, Anthony D. Joseph, Benjamin I. P. Rubinstein, Udam Saini, Charles Sutton, J. D. Tygar, and Kai Xia. 2008. Exploiting machine learning to subvert your spam filter. In *LEET'08: Proceedings of the 1st Usenix Workshop on Large-Scale Exploits and Emergent Threats*. USENIX Association, Berkeley, CA, USA, 1–9.
- [27] Andrew Newell, Rahul Potharaju, Luojie Xiang, and Cristina Nita-Rotaru. 2014. On the Practicality of Integrity Attacks on Document-Level Sentiment Analysis. In *Proc. Workshop on Artificial Intelligence and Security (AISec)*.
- [28] James Newsome, Brad Karp, and Dawn Song. 2006. Paragraph: Thwarting signature learning by training maliciously. In *Recent advances in intrusion detection*. Springer, 81–105.
- [29] Nicolas Papernot, Patrick McDaniel, and Ian Goodfellow. 2016. Transferability in Machine Learning: from Phenomena to Black-Box Attacks using Adversarial Samples. *arXiv:1605.07277*. (2016).
- [30] Nicolas Papernot, Patrick McDaniel, Ian Goodfellow, Somesh Jha, Z. Berkay Celik, and Ananthram Swami. 2017. Practical Black-Box Attacks Against Machine Learning. In *Proceedings of the 2017 ACM on Asia Conference on Computer and Communications Security (ASIA CCS '17)*. ACM, New York, NY, USA, 506–519.
- [31] Nicolas Papernot, Patrick D. McDaniel, and Ian J. Goodfellow. 2016. Transferability in Machine Learning: from Phenomena to Black-Box Attacks using Adversarial Samples. *ArXiv e-prints abs/1605.07277* (2016).
- [32] F. Pedregosa, G. Varoquaux, A. Gramfort, V. Michel, B. Thirion, O. Grisel, M. Blondel, P. Prettenhofer, R. Weiss, V. Dubourg, J. Vanderplas, A. Passos, D. Courville, M. Brucher, M. Perrot, and E. Duchesnay. 2011. Scikit-learn: Machine Learning in Python. *Journal of Machine Learning Research* 12 (2011), 2825–2830.
- [33] R. Perdisci, D. Dagon, Wenke Lee, P. Fogla, and M. Sharif. 2006. Misleading worm signature generators using deliberate noise injection. In *Proc. IEEE Security and Privacy Symposium (S&P)*.
- [34] Andrew Slavin Ross and Finale Doshi-Velez. 2018. Improving the Adversarial Robustness and Interpretability of Deep Neural Networks by Regularizing Their Input Gradients. In *AAAI AAAI Press*.
- [35] Benjamin I.P. Rubinstein, Blaine Nelson, Ling Huang, Anthony D. Joseph, Shing-hon Lau, Satish Rao, Nina Taft, and J. D. Tygar. 2009. ANTIDOTE: understanding and defending against poisoning of anomaly detectors. In *Proceedings of the 9th ACM SIGCOMM Internet Measurement Conference (IMC '09)*. ACM, New York, NY, USA, 1–14.
- [36] Paolo Russu, Ambra Demontis, Battista Biggio, Giorgio Fumera, and Fabio Roli. 2016. Secure Kernel Machines against Evasion Attacks. In *9th ACM Workshop on Artificial Intelligence and Security (AISec '16)*. ACM, New York, NY, USA, 59–69.
- [37] Mahmood Sharif, Sruti Bhagavatula, Lujo Bauer, and Michael K Reiter. 2016. Accessorize to a crime: Real and stealthy attacks on state-of-the-art face recognition. In *Proceedings of the 2016 ACM SIGSAC Conference on Computer and Communications Security*. ACM, 1528–1540.
- [38] C. J. Simon-Gabriel, Y. Ollivier, B. Schölkopf, L. Bottou, and D. Lopez-Paz. 2018. Adversarial Vulnerability of Neural Networks Increases with Input Dimension. *ArXiv e-prints* (2018).
- [39] J. Sokolić, R. Giryes, G. Sapiro, and M. R. D. Rodrigues. 2017. Robust Large Margin Deep Neural Networks. *IEEE Transactions on Signal Processing* 65, 16 (Aug 2017), 4265–4280.
- [40] Octavian Suciu, Radu Marginean, Yigitcan Kaya, Hal Daume III, and Tudor Dumitras. 2018. When Does Machine Learning FAIL? Generalized Transferability for Evasion and Poisoning Attacks. In *27th USENIX Security Symposium (USENIX Security '18)*. USENIX Association, Baltimore, MD, 1299–1316. <https://www.usenix.org/conference/usenixsecurity18/presentation/suciu>
- [41] Christian Szegedy, Wojciech Zaremba, Ilya Sutskever, Joan Bruna, Dumitru Erhan, Ian Goodfellow, and Rob Fergus. 2014. Intriguing properties of neural networks. In *International Conference on Learning Representations*. <http://arxiv.org/abs/1312.6199>
- [42] F. Tramèr, N. Papernot, I. Goodfellow, D. Boneh, and P. McDaniel. 2017. The Space of Transferable Adversarial Examples. *ArXiv e-prints* (2017).
- [43] D. Varga, A. Csiszár, and Z. Zombori. 2017. Gradient Regularization Improves Accuracy of Discriminative Models. *ArXiv e-prints ArXiv:1712.09936* (2017).
- [44] Nedom Šrndić and Pavel Laskov. 2014. Practical Evasion of a Learning-Based Classifier: A Case Study. In *Proc. 2014 IEEE Symp. Security and Privacy (SP '14)*. IEEE CS, Washington, DC, USA, 197–211.
- [45] Lei Wu, Zhanxing Zhu, Cheng Tai, and Weinan E. 2018. Enhancing the Transferability of Adversarial Examples with Noise Reduced Gradient. *ArXiv e-prints* (2018).
- [46] Huang Xiao, Battista Biggio, Gavin Brown, Giorgio Fumera, Claudia Eckert, and Fabio Roli. 2015. Is Feature Selection Secure against Training Data Poisoning?. In *JMLR W&CP - Proc. 32nd Int'l Conf. Mach. Learning (ICML)*, Francis Bach and David Blei (Eds.), Vol. 37. 1689–1698.
- [47] Weilin Xu, Yanjun Qi, and David Evans. 2016. Automatically Evading Classifiers A Case Study on PDF Malware Classifiers. In *Proceedings of the Network and Distributed System Security Symposium (NDSS)*. Internet Society.
- [48] F. Zhang, P.P.K. Chan, B. Biggio, D.S. Yeung, and F. Roli. 2016. Adversarial Feature Selection Against Evasion Attacks. *IEEE Transactions on Cybernetics* 46, 3 (2016), 766–777.

8 APPENDIX

In this appendix we report additional experiments for both evasion and poisoning on security datasets.

8.1 Transferability of Evasion Attacks for Malware Detection

We report here evasion experiments on the Drebin malware detection dataset. We report the evaluation of the classifier vulnerability in the white box scenario and the size of the input gradients in Fig. 14. The transferability between different models in black-box settings is shown in Fig. 15. The other two metrics that impact transferability include the cosine angle metric (Fig. 16) and the variance of the attacker objective function (Fig. 17). All the results

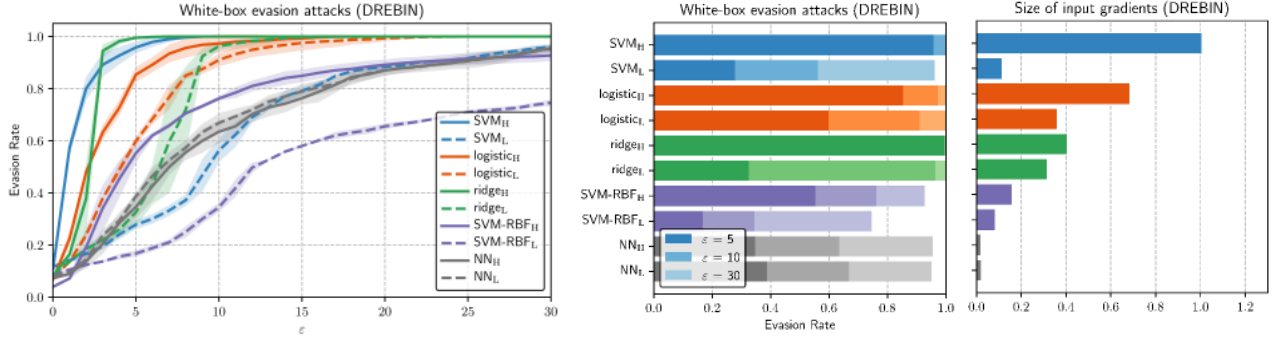


Figure 14: White-box evasion attacks on DREBIN. Test error as a function of the maximum perturbation $\epsilon \in [0, 30]$ (left). Test error for 3 levels of perturbation: $\epsilon \in \{5, 10, 30\}$ (middle). Average size of input gradients S (Eq. 17) for target classifiers (right).

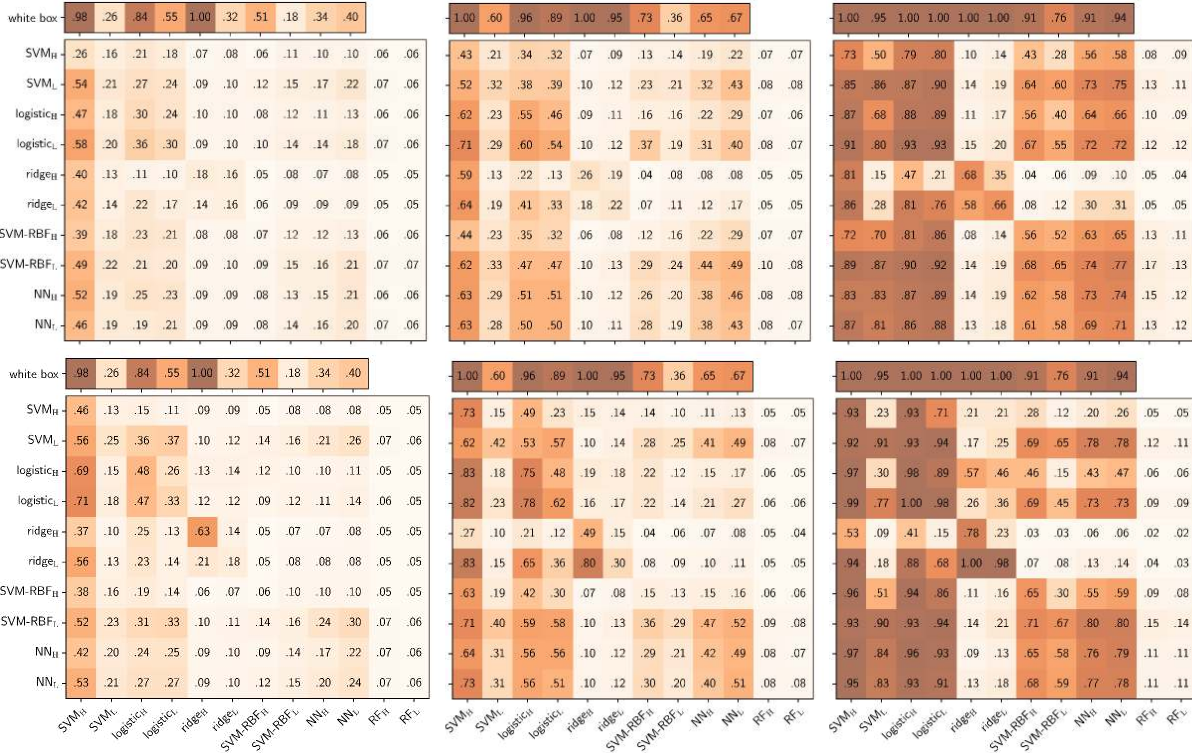


Figure 15: Transferability of black-box evasion results on DREBIN. Each cell in a matrix contains the test error of the target classifiers (in columns) on the attack samples crafted against the surrogate learners (in rows). Top row uses 20% training data, while bottom row uses 100% training data for surrogate model. The columns show test errors for different values of ϵ (5 left, 10 middle, and 30 right). Darker color means higher test error and indicates higher transferability.

confirm our findings on the MNIST89 dataset. The only notable difference is the vulnerability of random forests discussed in Sec. 5.

8.2 Transferability of Poisoning Attacks for Face Recognition

For the security analysis of classifiers against poisoning attacks we consider here a face recognition task on the Labeled Face on the Wild (LFW) dataset. We report the evaluation of the classifier vulnerability in the white box scenario and the size of the input

gradients in Fig. 18. The evaluation of transferability in the black-box scenario is in Fig. 19. The cosine angle metric and the correlation between the images is provided in Fig. 20, while the variance of the attacker objective function is given in Fig. 21. As for the MNIST89 dataset, in Fig. 22 we show some adversarial samples crafted against a classifier with three different levels of regularization. We observe that samples are perturbed proportionally to the regularization level of the classifier. These results confirm the main findings on the MNIST89 dataset.

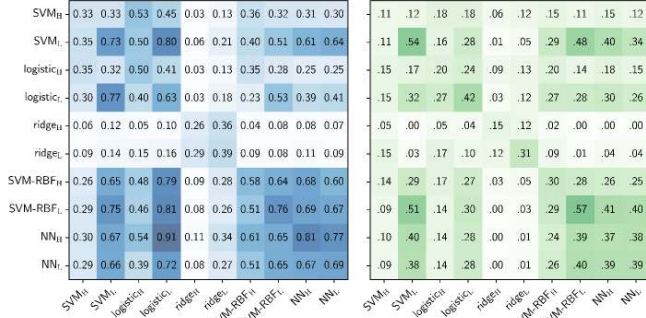


Figure 16: Gradient alignment R (Eq. 18) between surrogate (in rows) and target (in columns) classifiers, averaged on the unmodified test samples (left). Pearson correlation between perturbations on the DREBIN dataset for evasion (right).

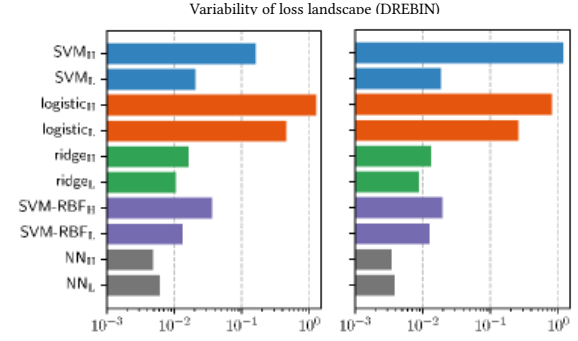


Figure 17: Variability V (Eq. 19) of the loss of the surrogate learner trained on DREBIN, with 20% (left) and 100% (right) training samples, averaged on the unmodified test samples.

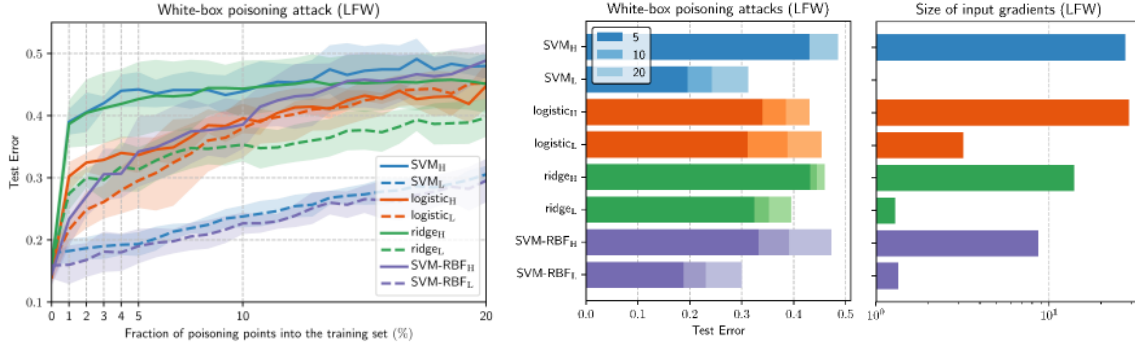


Figure 18: White-box poisoning attacks on LFW. Test error as a function of the percentage of poisoning points $\epsilon \in [5\%, 20\%]$ (left). Test error for three levels of poisoning rates: $\epsilon \in 5, 10, 20\%$ (middle). Average size of input gradients S (Eq. 17) for target classifiers (right).

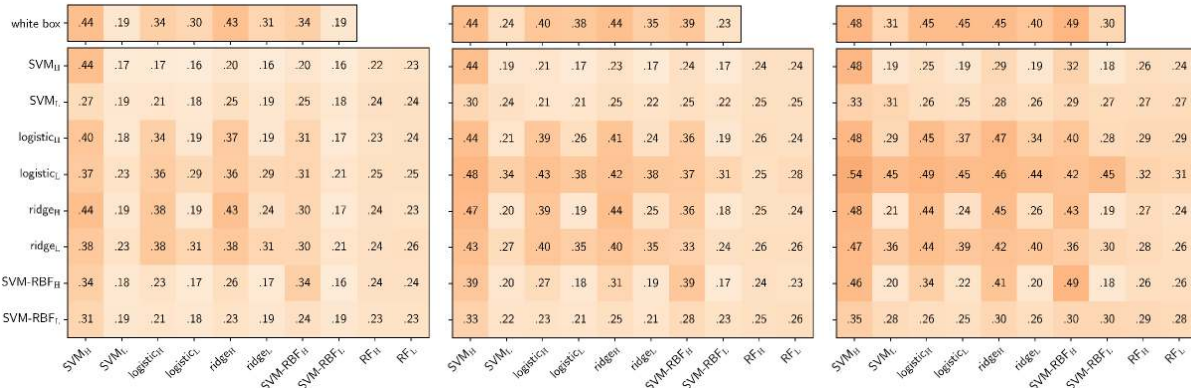


Figure 19: Transferability of black-box poisoning attacks on LFW. We report error for different percentages of poisoning (5% on left, 10% in the middle, and 20% on the right). The surrogate models are in the rows and the target models in the columns. Darker color means higher test error and indicates higher transferability.

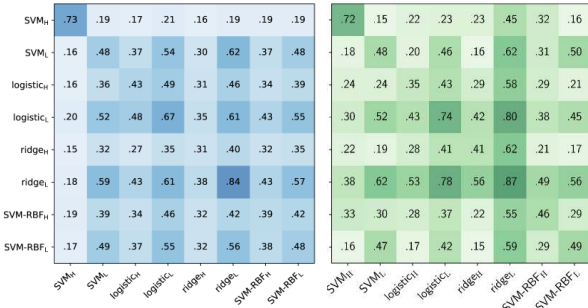


Figure 20: Gradient alignment R (Eq. 18) between surrogate (in rows) and target (in columns) classifiers, averaged on the unmodified test samples (left). Pearson correlation between perturbations on the LFW dataset for evasion (right).

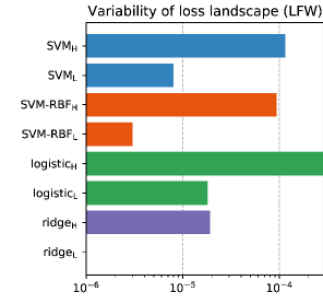


Figure 21: Variability V (Eq. 19) of the loss of the surrogate learner on LFW, averaged on different poisoning points.

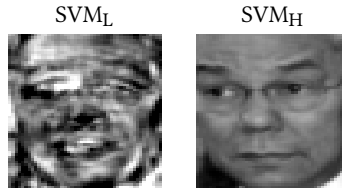


Figure 22: Adversarial examples crafted against linear SVMs. Larger perturbations are required to have significant impact on low-complexity classifiers (L), while minimal changes are very effective on high-complexity SVMs (H).